The Cardiac Conduction System

13

Timothy G. Laske, Maneesh Shrivastav, and Paul A. Iaizzo

Abstract

The intrinsic conduction system of the heart is comprised of several specialized subpopulations of cells that either spontaneously generate electrical activity (pacemaker cells) or preferentially conduct this activity throughout the chambers in a coordinated fashion. This chapter will discuss the details of this known anatomy as well as put such discoveries into a historical context. The cardiac action potential underlies signaling within the heart, and the various populations of myocytes will elicit signature waveforms. The recording or active sensing of these potentials is important in both research and clinical arenas. This chapter aims to present a basic understanding of the cardiac conduction system to provide the reader with a foundation for future research and reading on this topic. The information in this chapter is not comprehensive and should not be used to make decisions relating to patient care.

Keywords

Cardiac conduction • Sinoatrial node • Depolarization • Atrioventricular node • Electrophysiology • Cardiac action potential • Gap junction

Electronic supplementary material: The online version of this chapter (doi:10.1007/978-3-319-19464-6_13) contains supplementary material, which is available to authorized users. Videos can also be accessed at http://link.springer.com/book/10.1007/978-3-319-19464-6_13.

T.G. Laske, PhD (✉)
Department of Surgery, University of Minnesota, Minneapolis, MN, USA

Medtronic plc, 8200 Coral Sea Street NE, MVS 46, Minneapolis, MN 55112, USA
e-mail: tim.g.laske@medtronic.com

M. Shrivastav, PhD
Medtronic plc, 8200 Coral Sea Street NE, MVS 46, Minneapolis, MN 55112, USA

P.A. Iaizzo, PhD
Department of Surgery, University of Minnesota, Minneapolis, MN, USA

13.1 Introduction

Orderly contractions of the atria and ventricles are regulated by the transmission of electrical impulses that pass through an intricate network of modified cardiac muscle cells, the *cardiac conduction system*. These cells are interposed within the contractile myocardium. This intrinsic conduction system is comprised of several specialized subpopulations of cells that spontaneously generate electrical activity (pacemaker cells) and/or preferentially conduct this activity throughout the heart. Following an initiating activation (or depolarization) within the myocardium, this electrical excitation spreads throughout the heart in a rapid and highly coordinated fashion. This system of cells also functionally controls the timing

P.A. Iaizzo (ed.), *Handbook of Cardiac Anatomy, Physiology, and Devices*, DOI 10.1007/978-3-319-19464-6_13

of the transfer of activity between the atrial and ventricular chambers. Interestingly, a common global architecture is present in mammals, but significant interspecies differences exist at the histologic level [1, 2] (see also Chap. 6).

Discoveries relating to this intrinsic conduction system within the heart are relatively recent relative to cardiac function and anatomy. Johannes E. von Purkinje first described the ventricular conduction system in 1845 and Gaskell, an electrophysiologist, coined the phrase *heart block* in 1882. Importantly, Gaskell also related the presence of a slow ventricular rate to disassociation with the atria [3]. The discovery of the mammalian sinoatrial node was published by Sir Arthur Keith and Martin Flack in 1907 in the *Journal of Anatomy and Physiology*. Nevertheless, novel findings related to the functionality of this node are still being made today [4].

The elucidation of the bundle of His is attributed to its namesake, Wilhelm His Jr [5], who described the presence in the heart of a conduction pathway from the atrioventricular node through the cardiac skeleton that eventually connected to the ventricles. Tawara later verified the existence of the bundle of His in 1906 [6]. Due to the difficulty in distinguishing the atrioventricular nodal tissue from surrounding tissue, he defined the beginning of the bundle of His as the point at which these specialized atrioventricular nodal cells enter the central fibrous body (which delineates the atria from the ventricles). Tawara is also credited with being the first to clearly identify the specialized conduction tissues (modified myocytes) that span from the atrial septum to the ventricular apex, including the right and left bundle branches and Purkinje fibers.

Walter Karl Koch (1880–1962) was a distinguished German surgeon who discovered a triangular-shaped area in the right atrium of the heart that marks the atrioventricular node (known today as *Koch's triangle*). Among Koch's notable research findings was his hypothesis that the last part of the heart to lose activity when the whole organ died was the pacemaker region (*ultimum moriens*). Koch localized this last region of the heart to lose function through his detailed anatomical and histological studies of the hearts of animals and stillborn human fetuses. He postulated that the cardiac region near the opening of the wall of the coronary sinus was the true pacemaker of the heart [7, 8]; the atrioventricular node will elicit an escape rhythm when the sinoatrial node in the right atrium fails (see below).

Early discoveries by distinguished researchers such as Koch, Tawara, and Aschoff (to be discussed later in the text) have been immortalized in medical terminology (Koch's triangle, Tawara's node, and Aschoff's nodule). As history demonstrates, a thorough understanding of the anatomy and function of the cardiac conduction system is important for those designing cardiovascular devices and procedures. More specifically, surgical interventions (heart valve replacement/repair, repair of septal defects, coronary bypass grafting, congenital heart repair, etc.) are commonly associated with temporary or permanent heart block due to damage of the conduction system and/or disruption of its blood supply [9–13]. Hence, if one is designing corrective procedures and/or devices to be used, she/he needs to consider ways to avoid damage to cellular structures of the conduction system. For example, advances in surgical techniques for the repair of ventricular septal defects have reduced the incidence of complete atrioventricular block from 16 % in the 1950s to less than 1 % currently [14, 15]. Additionally, many rhythm control devices such as pacemakers and defibrillators aim to return the patient to a normal rhythm and contraction sequence [16–24]. Research has also continued relative to the repair or replacement of the intrinsic conduction system using gene and/or cell therapies [25].

A final example illustrating why an understanding of the heart's conduction system is critical to the design of devices and procedures is the therapeutic use of cardiac ablation. These methodologies purposely modify the heart to: (1) destroy portions of the conduction system (e.g., atrioventricular nodal ablation in patients with permanent atrial fibrillation), (2) eliminate aberrant pathways (e.g., accessory pathway ablation in Wolff–Parkinson–White syndrome), and/or (3) destroy inappropriate substrate behavior (e.g., ablation of ectopic foci or reentrant pathways in ventricular tachycardias, ablation for treatment of atrial fibrillation, etc.) [26–29].

13.2 Overview of Cardiac Conduction

The *sinoatrial node* is located in the right atrium in the healthy heart and serves as the natural pacemaker (Fig. 13.1). These pacemaker cells manifest spontaneous depolarizations and are thus responsible for generating the normal cardiac rhythm, also described as *intrinsic or automatic*. Importantly, the frequency of this earliest depolarization is modulated by both sympathetic and parasympathetic efferent innervation. In addition, the nodal rate can also be modulated by local changes associated with perfusion and/or the chemical environment (i.e., neurohormonal, nutritional, oxygenation, etc.). Although the atrial rhythms normally emanate from the sinoatrial node, variations in the initiation site of atrial depolarization have been documented outside of the histological nodal tissues, particularly when high atrial rates are elicited [30–33].

One of the most conspicuous features of sinoatrial nodal cells is that they possess poorly developed contractile apparati (a common feature to all myocytes specialized for conduction), comprising only about 50 % of the intracellular volume [34]. In general, although it cannot be seen grossly, the location of the sinoatrial node is on the "roof" of the right atrium at the approximate junction of the superior vena cava, the right atrial appendage, and the sulcus terminalis. In the adult human, the node is approximately 1 mm below the epicardium, 10–20 mm long and up to 5 mm thick [35]. For more details on cardiac anatomy, refer to Chaps. 5 and 6.

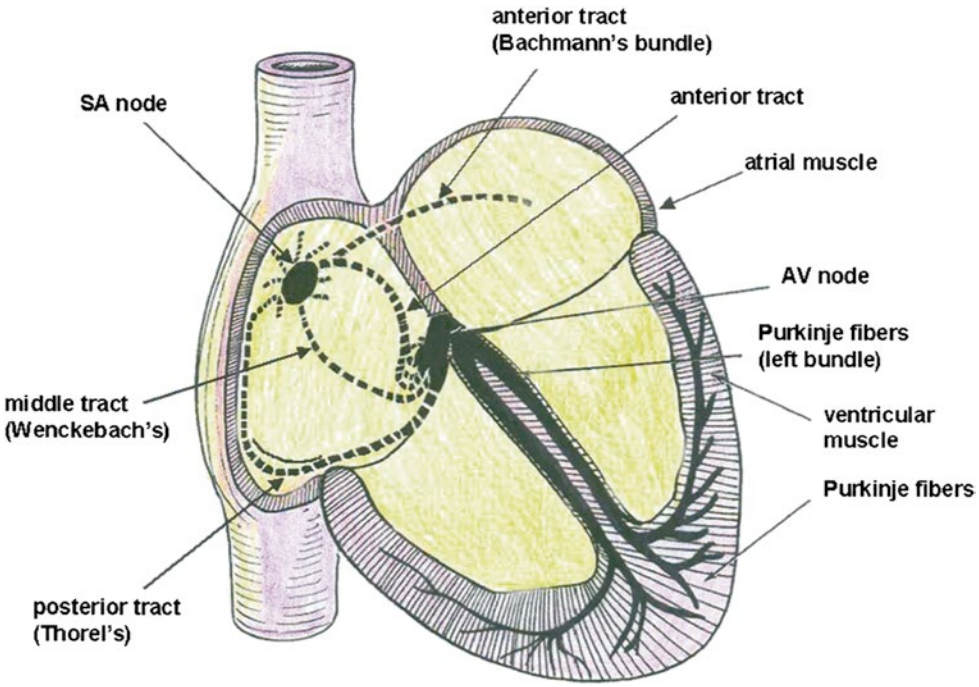

Fig. 13.1 Conduction system of the heart. Normal excitation originates in the sinoatrial node and then propagates through both atria (internodal tracts shown as *dashed lines*). The atrial depolarization spreads to the atrioventricular node and passes through the bundle of His (not labeled) and then to the Purkinje fibers which make up the left and right bundle branches; subsequently all ventricular muscle becomes activated. *AV* atrioventricular, *SA* sinoatrial

After initial sinoatrial nodal excitation, depolarization spreads throughout the atria. The exact mechanisms involved in the spread of impulses (excitation) from the sinoatrial node across the atria are somewhat controversial [36]. However, it is generally accepted that: (1) the spread of depolarizations from nodal cells can go directly to adjacent myocardial cells and (2) preferentially ordered myofibril pathways allow this excitation to rapidly transverse the right atrium to both the left atrium and the atrioventricular node. It is believed that there are three preferential anatomic conduction pathways from the sinoatrial node to the atrioventricular node (known as the node of Tawara) [37]. In general, these can be considered as the shortest electrical routes between the nodes. They are microscopically identifiable structures, appearing to be preferentially oriented fibers that provide a direct node-to-node pathway. In some hearts, pale staining Purkinje-like fibers have also been reported in these regions (tracts are shown as dashed lines in Fig. 13.1; also see Fig. 13.1 in the online supplemental material). More specifically, the anterior tract is described as extending from the anterior part of the sinoatrial node, bifurcating into the so-called Bachmann's bundle (delivering impulses to the left atrium) and a second tract that descends along the interatrial septum which connects to the anterior part of the atrioventricular node. The middle (or Wenckebach's pathway) extends from the superior part of the sinoatrial node, runs posteriorly to the superior vena cava, then descends within the atrial septum, and may join the anterior bundle as it enters the atrioventricular node. The third pathway is described as being posterior (Thorel's) which, in general, is considered to extend from the inferior part of the sinoatrial node, passing through the crista terminalis and the Eustachian valve past the coronary sinus to enter the posterior portion of the atrioventricular node. In addition to excitation along these preferential conduction pathways, general excitation spreads from cell to cell throughout the entire atrial myocardium via the specialized connections between cells, the *gap junctions*, which exist between all myocardial cell types (see below).

Toward the end of atrial depolarization, the excitatory signal reaches the atrioventricular node. This excitation reaches these cells via the aforementioned atrial routes, with the final excitation of the atrioventricular node generally described as occurring via the slow or fast pathways. The slow and fast pathways are functionally, and usually anatomically, distinct routes to the atrioventricular node. The slow pathway generally crosses the isthmus between the coronary sinus and the tricuspid annulus and has a longer conduction time but a shorter effective refractory period than the fast pathway. The fast pathway is commonly a superior route, emanating from the interatrial septum, and has a faster conduction rate but, in turn, a longer effective refractory period. Normal conduction during sinus rhythm occurs along the fast pathway, but higher heart rates and/or premature beats are often conducted through the slow pathway, since the fast pathway may be refractory at these rates.

Recent advances in the optical mapping of the human atrioventricular junction further elucidate the dual pathway electrophysiology [38]. More specifically, the dual characteristics of this function have been revealed using an S1–S2 pacing protocol; in this procedure, a stimulus (S1) of constant

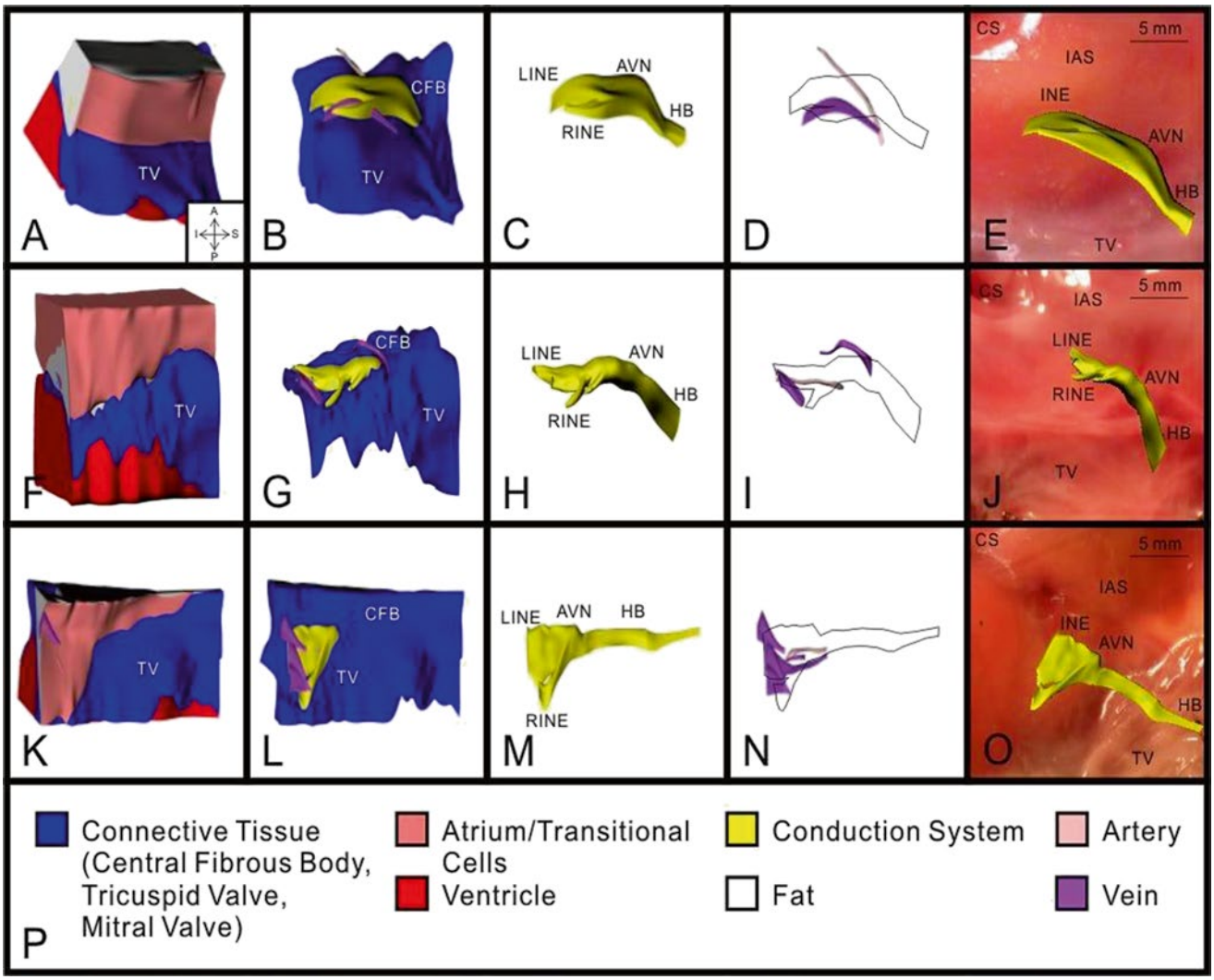

Fig. 13.2 3D reconstruction of atrioventricular (AV) junction from three human hearts: heart #1 (**A**–**E**), heart #2 (**F**–**J**), and heart #3 (**K**–**O**). **A**, **F**, and **K**: complete 3D reconstruction with all types of tissue visible. **B**, **G**, and **L**: 3D reconstruction with areas of atrium, ventricle, and fat removed. **C**, **H**, and **M**: 3D reconstruction of conduction system. **D**, **I**, and **N**: 3D reconstruction of major veins and arteries with conduction system outlined. **E**, **J**, and **O**: 3D reconstruction of conduction system superimposed on a photograph of the tissue used for its creation. **P**: key to the colors in **A**–**O**. *AVN* atrioventricular node, *CFB* central fibrous body, *HB* His bundle, *LINE* leftward inferior nodal extension, *RINE* rightward inferior nodal extension, *TV* tricuspid valve

duration and amplitude is applied followed by a second stimulus (S2) of varying duration and amplitude. The S1–S2 interval is iteratively reduced until conduction block in the fast pathway occurs due to the long refractory period [38].

Though the primary function of the atrioventricular node may seem simple, that is, to relay conduction between the atria and ventricles, its structure is very complex. As a means to describe these complexities, mathematical arrays and finite element analysis models have been constructed to elucidate the underlying structure–function relationship of the node [39]. Figure 13.2 shows a 3D reconstruction of the region using a model of the heart stained with the voltage sensitive dye di-4-ANEPPS. The reconstruction includes histological and immunolabeling of marker proteins to identify various tissue types. Figure 13.3 shows the nodal reconstruction of a normal human heart as well as one from a patient who had an implanted left ventricular assist device. For examples of these reconstructions, see Videos 13.1, 13.2, and 13.3 in the online supplemental material.

In general, the atrioventricular node is located in the so-called floor of the right atrium, over the muscular part of the interventricular septum and inferior to the membranous septum. Following atrioventricular nodal excitation, impulses are conducted to the His bundle (note that the bundle of His has also been referred to as the *common bundle* or *His bundle*). If conduction follows the slow pathway, a longer interval is present between atrial and His activation. As mentioned above, the anatomical region in which the His bundle and the

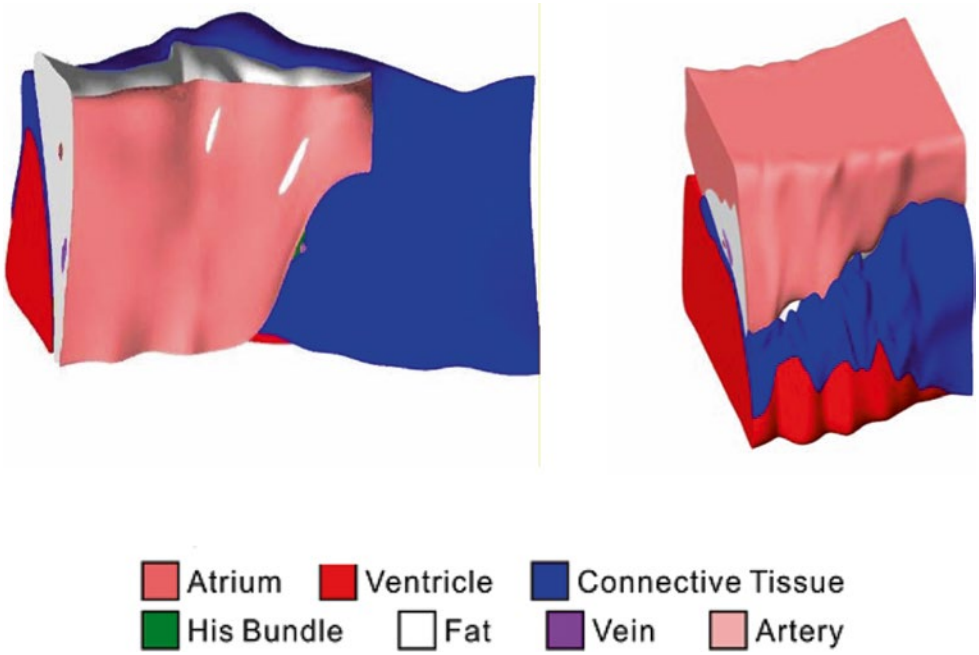

Fig. 13.3 Atrioventricular reconstruction with normal and pathologic human hearts. The normal human heart (*left*) and the heart of a left ventricular assist device patient (*right*) show different proportions of tissue type in the nodal region

atrioventricular node both reside has been termed the *triangle of Koch*. The triangle is bordered by the coronary sinus, the tricuspid valve annulus along the septal leaflet, and the tendon of Todaro.

After leaving the bundle of His, the normal wave of cardiac depolarization spreads to both the left and right bundle branches; these pathways carry depolarization to the left and right ventricles, respectively. Finally, the signal broadly travels through the remainder of the Purkinje fibers and ventricular myocardial depolarization spreads (see Video 13.4 in the online supplemental material).

In addition to the normal path of ventricular excitation, direct connections to the ventricular myocardium from the atrioventricular node and the penetrating portion of the bundle of His have been described in humans [40]. The function and prevalence of these connections, termed *Mahaim fibers*, is poorly understood. An additional aberrant pathway existing between the atria and ventricles has been termed the *bundle of Kent* (the clinical manifestation of ventricular tachycardia due to the presence of this pathway is termed *Wolff–Parkinson–White syndrome*); this pathway is commonly ablated.

Alternate representations of the cardiac conduction system are shown in Figs. 13.4 and 13.5. Details of the ventricular portion of the conduction system are shown in Fig. 13.6. More specifically, the left bundle branch splits into fascicles as it travels down the left side of the ventricular septum just below the endocardium (these can be visualized with proper staining). Its fascicles extend for a distance of 5–15 mm, fanning out over the left ventricle. Importantly, typically about midway to the apex of the left ventricle, the left bundle separates into two major divisions, the anterior and posterior branches (or fascicles). These divisions extend to the base of

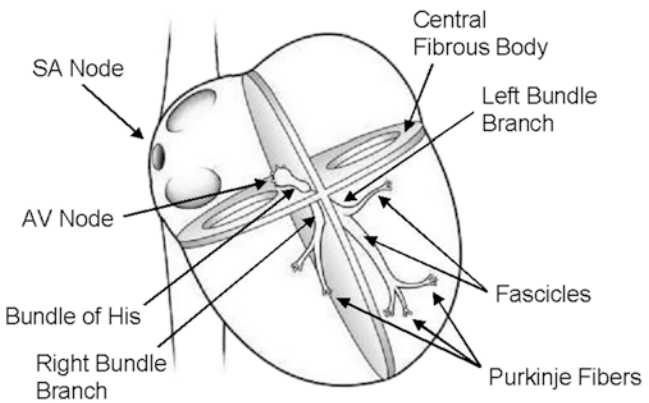

Fig. 13.4 Conduction system of the heart. Normal excitation originates in the sinoatrial node then propagates through both atria. The atrial depolarization spreads to the atrioventricular node and passes through the bundle of His to the bundle branches/Purkinje fibers. *AV* atrioventricular, *SA* sinoatrial

the two papillary muscles and the adjacent myocardium. In contrast, the right bundle branch continues inferiorly, as if it were a continuation of the bundle of His, traveling along the right side of the muscular interventricular septum. This bundle branch runs proximally just deep to the endocardium, and its course runs slightly inferior to the septal papillary muscle of the tricuspid valve before dividing into fibers that spread throughout the right ventricle. The complex network of conducting fibers that extends from either the right or left bundle branches is composed of the rapid conduction cells known as *Purkinje fibers*. The Purkinje fibers in both the right and left ventricles act as preferential conduction pathways to provide rapid activation and coordinate the excitation pattern within

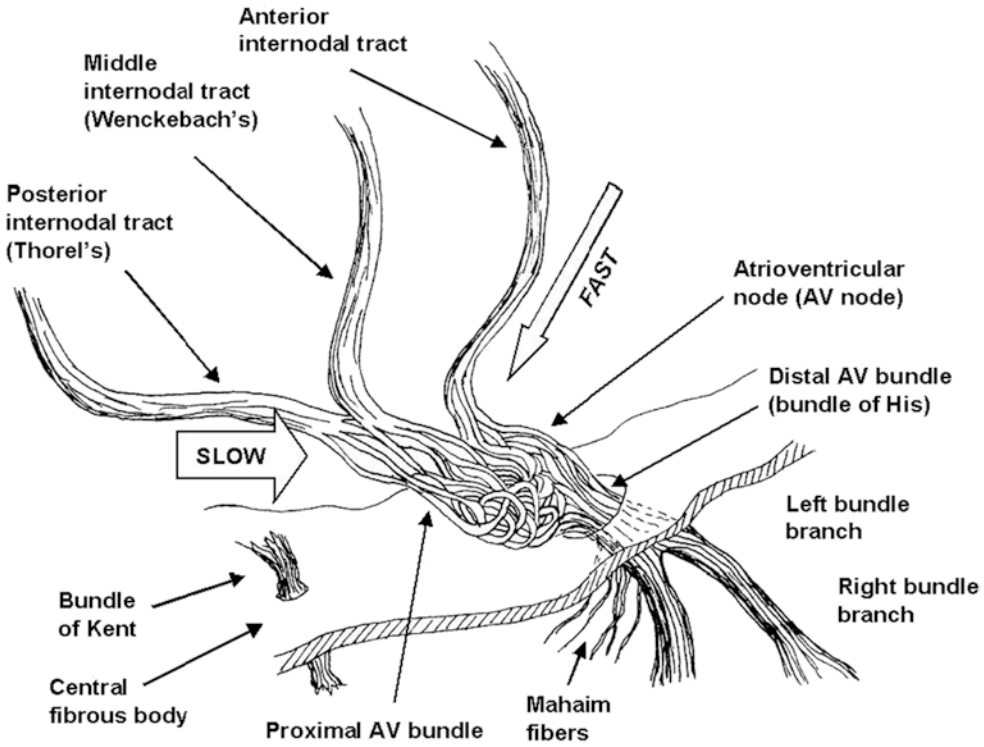

Fig. 13.5 Details of the atrioventricular nodal region. The so-called slow and fast conduction pathways are indicated by the *arrows*. To improve clarity in the visualization of the conduction anatomy, the fascicles of the atrioventricular node are not drawn to scale (their size was increased to allow the reader to visualize the tortuosity of the conduction pathway) and the central fibrous body has been thinned. *AV* atrioventricular

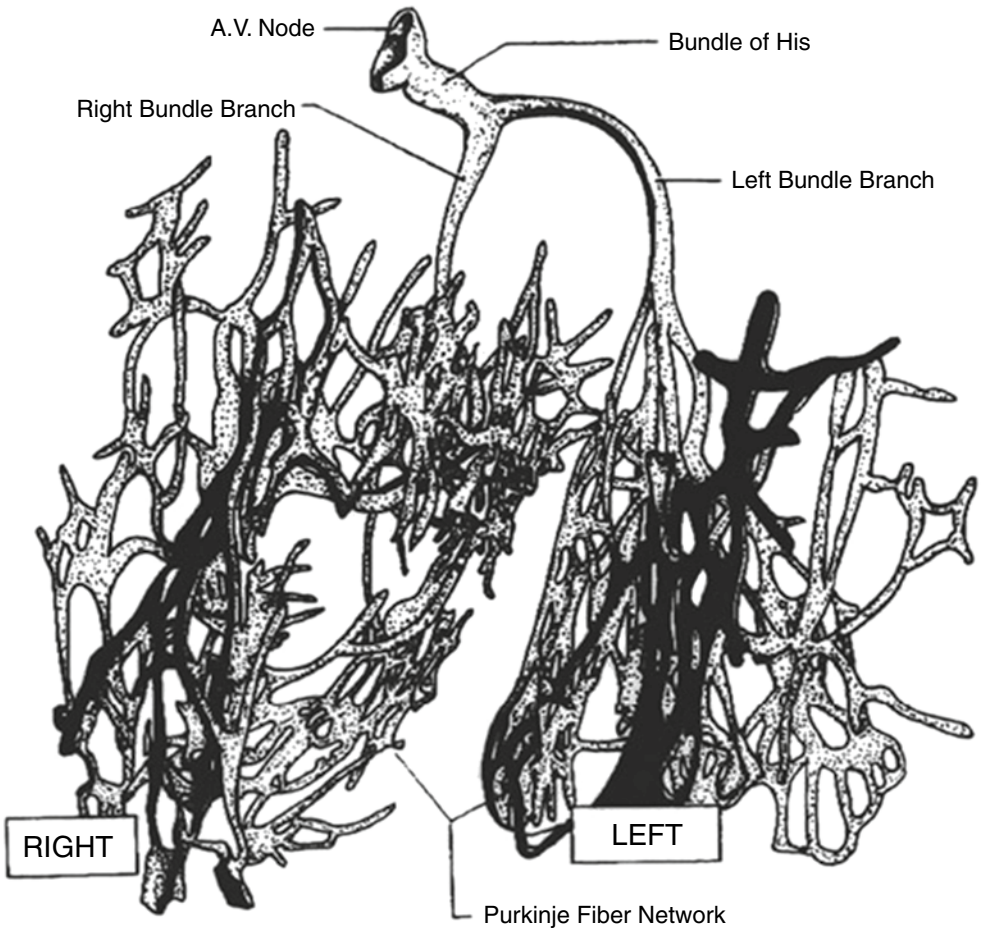

Fig. 13.6 Ventricular conduction system. The Purkinje network has a high interspecies and intraspecies variation, which likely results in variability in excitation and contractile patterns within the ventricles. This variability is evident in the dramatic differences seen in the degree and morphology of the cardiac trabeculations (which typically contain these fibers). Modified from DeHann DL, Circulation 1961; 24:458)

the various regions of the ventricular myocardium. As described by Tawara, these fibers travel within the trabeculations of the right and left ventricles, as well as within the myocardium. Due to the tremendous variability in the degree and morphology of trabeculations existing within and between species, it is likely that variations in the left ventricular conduction patterns also exist. It should be noted that one of the most easily recognized conduction pathways found in mammalian hearts is the moderator band, which contains Purkinje fibers from the right bundle branch (see also Chap. 6).

Three criteria for considering a myocardial cell as a *specialized conduction cell* were first proposed by Aschoff [41] and Monckeburg [42] in 1910, which include: (1) cells with the ability to histologically identify discrete features; (2) cells with the ability to track cells from section to section; and (3) these cells are insulated by fibrous sheaths from the nonspecialized contractile myocardium. It is noteworthy that only the cells within the bundle of His, the left and right bundle branches, and the Purkinje fibers satisfy all three criteria. No structure within the atria meets all three criteria, including Bachmann's bundle, the sinoatrial node, and the atrioventricular node (which are all uninsulated tissues).

13.3 Cardiac Rate Control

Under normal physiologic conditions, the dominant pacemaker of the heart is the sinoatrial node which, in adults, fires at rates between 60 and 100 beats per minute, faster than any other cardiac region. In an individual at rest, modulation by the parasympathetic nervous system dominates which slows the sinoatrial nodal rate to about 75 action potentials per minute (or beats per minute when contractions are elicited).

In addition to the cells of the sinoatrial node, other specialized conduction system cells are capable of developing spontaneous diastolic depolarization, specifically those found in the specialized fibers in the atrioventricular junction and His–Purkinje system. Rhythms generated by impulse formation within these cells range from 25 to 55 beats per minute in the human heart (Fig. 13.7). These lower-rate rhythms are commonly referred to as *ventricular escape rhythms* and are important for patient survival, since they maintain some degree of cardiac output in situations when the sinoatrial and/or atrioventricular nodes are nonfunctional or are functioning inappropriately. Note that the various populations of pacemaker myocytes (i.e., in the sinoatrial and atrioventricular nodes) elicit so-called slow-type action potentials (slow-response action potential; see below).

In addition to the normal sources of cardiac rhythm, myocardial tissue can also exhibit abnormal self-excitability; such a site is also called an *ectopic pacemaker* or *ectopic focus*. This pacemaker may operate only occasionally, producing extra beats, or it may induce a new cardiac rhythm for some period of time. Potentiators of ectopic activity include caffeine, nicotine, electrolyte imbalances, hypoxia, and/or toxic reactions to drugs such as digitalis. For more detail on rate control of the heart, refer to Chap. 14.

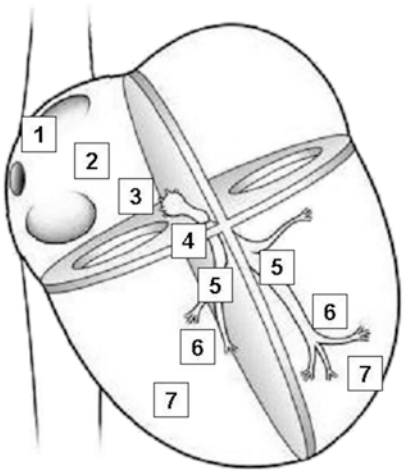

Normal Activation Sequence	Structure	Conduction velocity (m/sec)	Pacemaker rate (beats/min)
1	SA node	< 0.01	60 – 100
2	Atrial myocardium	1.0 – 1.2	None
3	AV node	0.02 – 0.05	40 – 55
4	Bundle of His	1.2 – 2.0	25 – 40
5	Bundle branches	2.0 – 4.0	25 – 40
6	Purkinje network	2.0 – 4.0	25 – 40
7	Ventricular myocardium	0.3 – 1.0	None

Fig. 13.7 Conduction velocities and intrinsic pacemaker rates of various structures within the cardiac conduction pathway. The structures are listed in the order of activation during a normal cardiac contraction, beginning with the sinoatrial node. Note that the intrinsic pacemaker rate is slower in structures further along the activation pathway. For example, the atrioventricular nodal rate is slower than the sinoatrial nodal rate. This prevents the atrioventricular node from generating a spontaneous rhythm under normal conditions, since it remains refractory at rates <55 beats per minute. If the sinoatrial node becomes inactive, the atrioventricular nodal rate will then determine the ventricular rate. Tabulation adapted from Katz AM (ed), Physiology of the Heart, 3rd edn., 2001)

13.4 Cardiac Action Potentials

Although cardiac myocytes branch and interconnect with each other (mechanically via the intercalated disk and electrically via the gap junctions), under normal conditions, the heart is thought to form two separate functional networks—the atria and the ventricles. The atrial and ventricular tissues are separated by the fibrous skeleton of the heart (the central fibrous body). This skeleton is comprised of dense connective tissue rings that surround the valves of the heart, fuse with one another, and merge with the interventricular septum. The skeleton can be considered to (1) form the foundation to which the valves attach, (2) prevent overstretching of the valves, (3) serve as a point of insertion for cardiac muscle bundles, and (4) act as an electrical insulator that prevents the direct spread of action potentials from the atria to the ventricles. See also Chap. 5 for further details on the cardiac skeleton.

A healthy myocardial cell has a resting membrane potential of approximately −90 mV. The resting potential is described by the Goldman–Hodgkin–Katz equation, which takes into account the permeabilities (Ps) as well as the intracellular and extracellular concentrations of ions [X], where X is the ion:

$$V_m = (2.3R*T/F)*\log_{10}\frac{P_K[K]_o + P_{Na}[Na]_o + P_{Cl}[Cl]_i + \ldots}{P_K[K]_i + P_{Na}[Na]_i + P_{Cl}[Cl]_o + \ldots}$$

In the cardiac myocyte, the membrane potential is dominated by the K^+ equilibrium potential. An action potential is initiated when this resting potential becomes shifted toward a more positive value of approximately −60 to −70 mV (Fig. 13.8). At this threshold potential, the cell's voltage-gated Na^+ channels open and begin a cascade of events involving other ion channels. In artificial electrical stimulation, this shift of the resting potential and subsequent depolarization is produced by the excitation delivered through the pacing system. The typical ion concentrations for a mammalian cardiac myocyte are summarized in Table 13.1 and graphically depicted in Fig. 13.9.

When a myocyte is brought to the threshold potential, normally via a neighboring cell, voltage-gated fast Na^+ channels actively open (activation gates); the permeability of the sarcolemma (plasma membrane) to sodium ions (P_{Na^+}) dramatically increases. Because the cytosol is electrically more negative than extracellular fluid, and the Na^+ concentration is higher in the extracellular fluid, Na^+ rapidly crosses the cell membrane. Importantly, within a few milliseconds, these fast Na^+ channels automatically inactivate (inactivation gates) and P_{Na^+} decreases.

The membrane depolarization due to the activation of the Na^+ induces the opening of the voltage-gated slow Ca^{2+} channels located within both the sarcolemma and sarcoplasmic reticulum (internal storage site for Ca^{2+}) membranes.

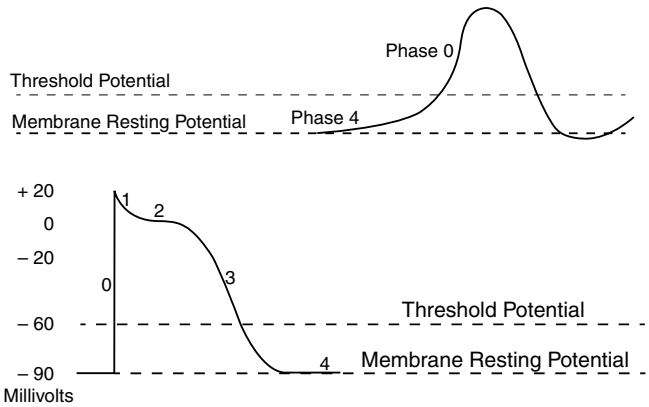

Fig. 13.8 Typical cardiac action potentials (slow on top and fast below). The resting membrane potential, the threshold potential, and the phases of depolarization (0–4) are shown

Table 13.1 Ion concentrations for mammalian myocytes

Ion	Intracellular concentration (mM)	Extracellular concentration (mM)
Sodium (Na)	5–34	140
Potassium (K)	104–180	5.4
Chloride (Cl)	4.2	117
Calcium (Ca)	–	3

Adapted from Katz AM (ed), Physiology of the Heart, 3rd edn., 2001

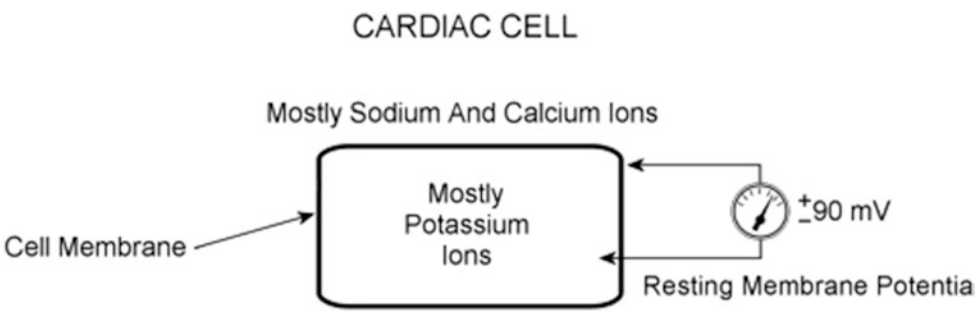

Fig. 13.9 Cardiac cell at rest. The intracellular space is dominated by potassium ions, while the extracellular space has a higher concentration of sodium and calcium ions

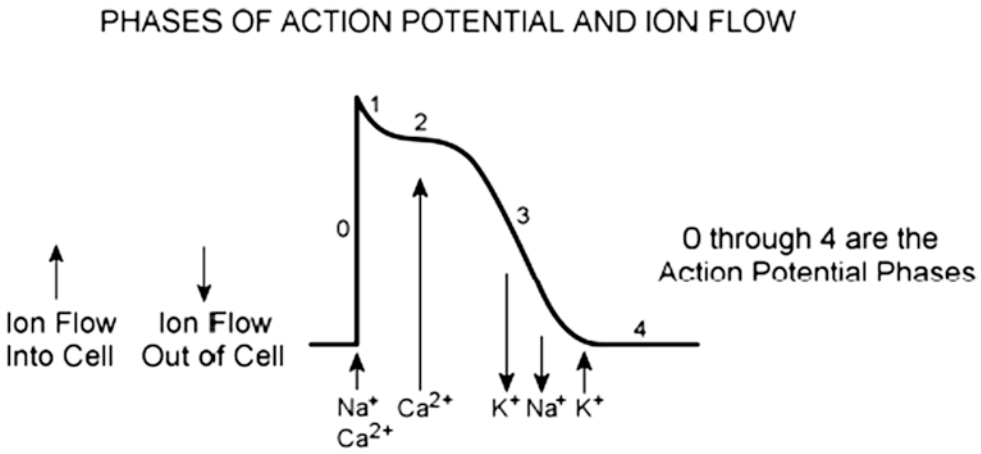

Fig. 13.10 Ion flow during the phases of a cardiac action potential

Thus, there is an increase in the permeability of Ca^{2+} ($P_{Ca^{2+}}$), which allows the concentration to dramatically increase intracellularly (Fig. 13.10). At the same time, the membrane permeability to K^+ ions decreases due to closing of K^+ channels. For approximately 200–250 ms, the membrane potential stays close to 0 mV, as a small outflow of K^+ just balances the inflow of Ca^{2+}. After this fairly long delay, voltage-gated K^+ channels open and active repolarization is initiated. The opening of these K^+ channels (increased membrane permeability) allows for K^+ to diffuse out of the cell due to its concentration gradient. At this same time, Ca^{2+} channels begin to close, and net charge movement is dominated by the outward flux of the positively charged K^+, restoring the negative resting membrane potential to approximately –90 mV (Figs. 13.10 and 13.11).

As mentioned above, not all action potentials that are elicited in the cardiac myocardium have the same time course; slow- and fast-response cells have differing shaped action potentials with different electrical properties in each phase. Recall that the pacemaker cells (slow-response type) have the ability to spontaneously depolarize until they reach threshold and thus elicit action potentials. Action potentials from such cells are also characterized by a slower initial depolarization phase, a lower amplitude overshoot, a shorter and less stable plateau phase, and repolarization to an unstable, slowly depolarizing resting potential (Fig. 13.12). In the pacemaker cells, at least three mechanisms are thought to underlie the slow depolarization that occurs during phase 4 (diastolic interval): (1) a progressive decrease in P_{K^+}, (2) a slight increase in P_{Na^+}, and (3) an increase in $P_{Ca^{2+}}$.

13.5 Gap Junctions (Cell-to-Cell Conduction)

In the heart, cardiac muscle cells (myocytes) are connected end to end by structures known as *intercalated disks*. These are irregular transverse thickenings of the sarcolemma, within which there are *desmosomes* that hold the cells together and to which the myofibrils are attached. Adjacent to the intercalated disks are the gap junctions, which allow action potentials to directly spread from one myocyte to the next. More specifically, the disks join the cells together by both mechanical attachment and protein channels. The firm mechanical connections are created between the adjacent cell membranes by proteins called adherins in the desmosomes. The electrical connections (low-resistance pathways, gap junctions) between the myocytes are via the channels formed by the protein connexin. These channels allow ion movements between cells (Fig. 13.13).

As noted above, not all cells elicit the same type of action potentials, even though excitation is propagated from cell to cell via their interconnections (gap junctions). The action potentials elicited in the sinoatrial nodal cells are of the slow-response type and those in the remainder of the atria have a more rapid depolarization rate (Fig. 13.14). Although a significant temporal displacement in the action potentials elicited by the myocytes of the two nodes (sinoatrial and atrioventricular) occurs, the action potential morphologies are similar.

It takes approximately 30 ms for excitation to spread between the sinoatrial and atrioventricular nodes, and atrial activation occurs over a period of approximately 70–90 ms (Fig. 13.14). The speed at which an action potential propagates through a region of cardiac tissue is called the *conduction velocity* (Fig. 13.7). The conduction velocity varies considerably in the heart and is directly dependent on the diameter of a given myocyte. For example, action potential conduction is greatly slowed as it passes through the atrioventricular node. This is due to the small diameter of these nodal cells, the tortuosity of the cellular pathway [2], and the slow rate of rise of their elicited action potentials. This delay is important to allow adequate time for ventricular filling.

Action potentials in the Purkinje fibers are of the fast-response type (Fig. 13.14), i.e., rapid depolarization rates that, in part, are due to their large diameters. This feature

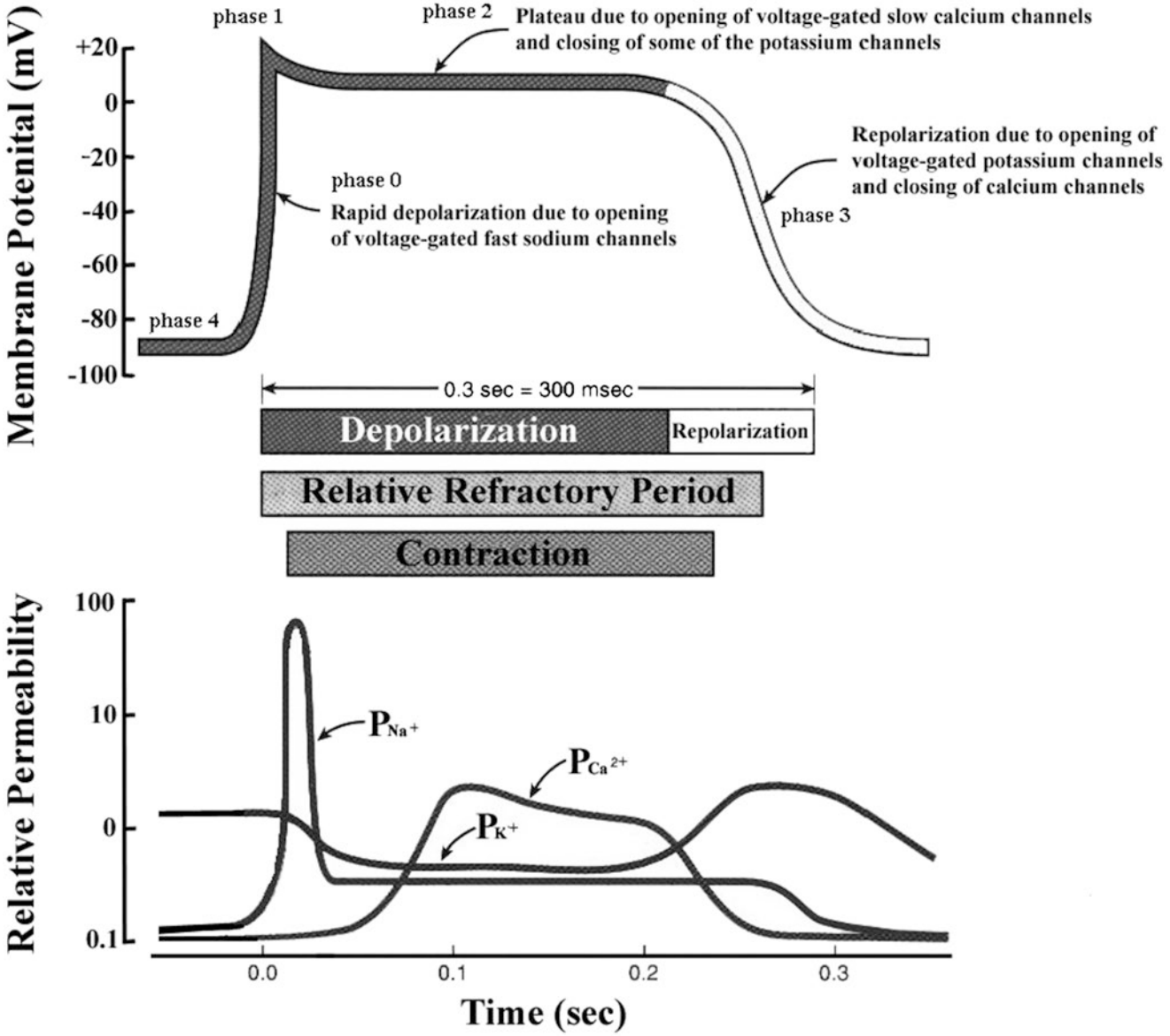

Fig. 13.11 A typical action potential of a ventricular myocyte and the underlying ion currents. The resting membrane potential is approximately −90 mV (phase 4). The rapid depolarization is primarily due to the voltage-gated Na^+ current (phase 0), which results in a relatively sharp peak (phase 1) and transitions into the plateau (phase 2) until repolarization (phase 3). Also indicated are the refractory period and timing of the ventricular contraction. Modified from Tortora GJ, Grabowski SR (eds), Principles of Anatomy and Physiology, 9th edn., 2000

allows the Purkinje system to transfer depolarization to the majority of cells in the ventricular myocardium nearly in unison. Because of the high conduction velocity in these cells which span the myocardium, there is a minimal delay in the cell's time of onset. It is important to note that the ventricular cells that are last to depolarize have shorter duration action potentials (shorter Ca^{2+} current) and thus are the first to repolarize. The ventricular myocardium repolarizes within the time period represented by the T-wave in the electrocardiogram.

13.6 The Atrioventricular Node and Bundle of His: Specific Features

The atrioventricular node and the bundle of His play critical roles in the maintenance and control of ventricular rhythms. As mentioned previously, the atrioventricular node is composed of heterogeneous gap junctions with electrical communication via the protein connexin. Specifically, there are four connexin proteins identified to date: Cx43, Cx40, Cx45, and Cx30.2/31.9. Cx43 and Cx40 are associated with the fast

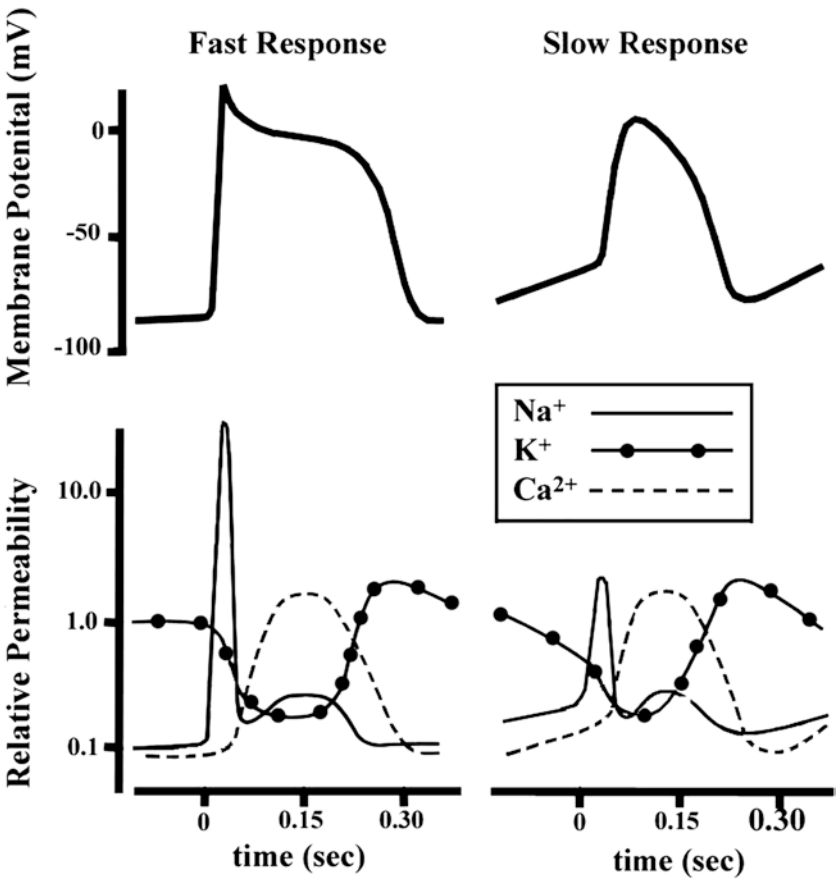

Fig. 13.12 The comparative time course of membrane potentials and ion permeabilities that would typically occur in a fast-response (*left*: ventricular myocyte) and a slow-response cell (*right*: nodal myocyte). Modified from Mohrman DE, Heller LJ (eds) Cardiovascular Physiology, 5th edn., 2003

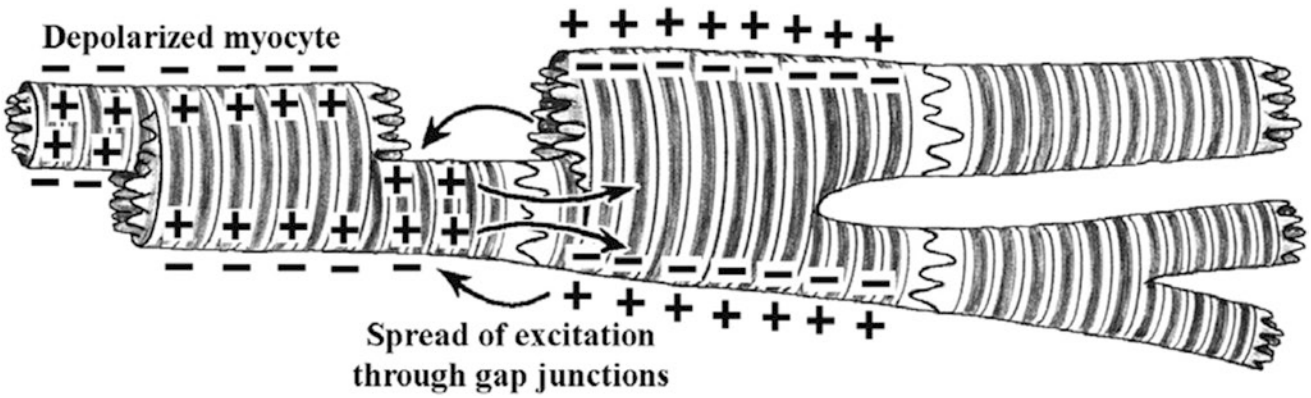

Fig. 13.13 Several cardiac myocytes in different states of excitation. The depolarization that occurred in the cell on the left causes depolarization of the adjacent cell through cell-to-cell conduction via the gap junctions (nexus). Eventually all adjoining cells will depolarize. An action potential initiated in any of these cells will be conducted from cell to cell in either direction

conduction pathway, whereas Cx45 and Cx30.2/31.9 are generally expressed in the slow conduction pathway [43]. The expression of these proteins is also species dependent; it should be noted that one study found Cx43, Cx40, and Cx45 are expressed in the human atrioventricular junction [44].

Additionally, both structures are frequently accessed during cardiac catheterization procedures: (1) as anatomic landmarks, (2) to allow insight into atrial–ventricular conduction behaviors, and/or (3) to ablate these structures or the surrounding tissues to terminate aberrant behaviors (e.g., reentrant tachycardias) or to prevent atrioventricular conduction in patients with chronic atrial fibrillation. Today, there is a strong interest by the medical device designer to understand the details of the structural and functional properties of the atrioventricular node and the bundle of His to develop new therapies and/or to avoid inducing complications.

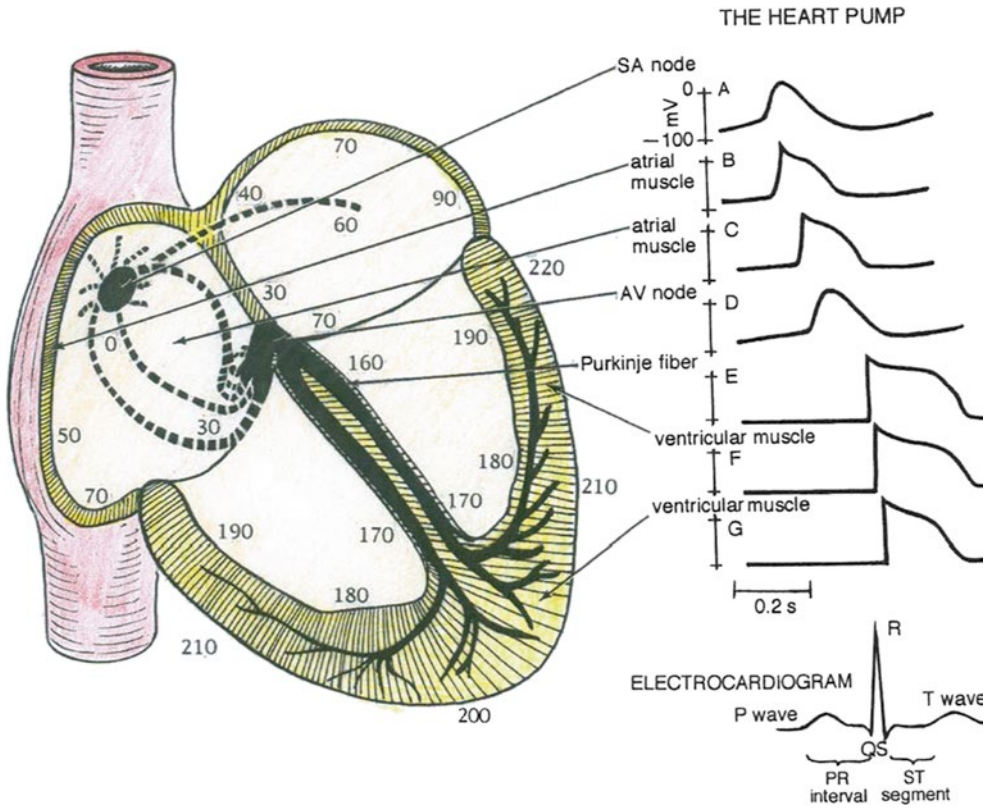

Fig. 13.14 Predominant conduction pathways in the heart and the relative time, in ms, that cells in these various regions become activated following an initial depolarization within the sinoatrial node. To the right are typical action potential waveforms that would be recorded from myocytes in these specific locations. The sinoatrial and atrioventricular nodal cells have similar shaped actions potentials. The non-pacemaker atrial cells elicit action potentials that have shapes somewhat between the slow-response (nodal) and fast-response cells (e.g., ventricular myocytes). The ventricular cells elicit fast-response-type action potentials; however, their durations vary in length. Due to the rapid excitation within the Purkinje fiber system, the initiation of depolarization of the ventricular myocytes occurs within 30–40 ms and is recorded as the QRS complex in the electrocardiogram

The myocytes located within the region of the atrioventricular node and the bundle of His have many unique characteristics. Specifically, both the atrioventricular node and His bundle are comprised primarily of "spiraled" myofibers that are then combined to form many collagen-encased fascicles. These fascicles are generally arranged in a parallel fashion in the proximal atrioventricular bundle (PAVB, the region of the atrioventricular node transitioning from the atrium into the body of the nodal tissues) and the distal atrioventricular bundle (DAVB, the penetrating portion of the bundle of His) and are interwoven within the atrioventricular node itself (the tortuosity of the cellular pathway within the atrioventricular node likely is a major contributor to the conduction delay in this region; Fig. 13.5). In general, the myocytes of the His are larger than those of the PAVB and the atrioventricular node, and the perinuclear regions of these myocytes are filled with glycogen. These cells uniquely utilize anaerobic metabolism instead of the normal aerobic metabolism used by the more abundant contractile myocardium. His myocytes have longer intercalated disks and, although all of the nodal tissues have thin end processes, they are less numerous in the His. His myocytes are innervated, but to a lesser extent than those in the atrioventricular node. Unlike the sinoatrial and atrioventricular nodes, the His bundle has no large blood vessels that supply it specifically. Table 13.2 provides a summary of histological characteristics of the His in comparison to the other nodal tissues.

It should be noted that the bundle of His can receive inputs from both the atrioventricular node and from transitional cells in the atrial septum. In general, the His bundle is located adjacent to the annulus of the tricuspid valve, distal to the atrioventricular node and slightly proximal to the right bundle branch and left bundle branch. The functional origin may be ill defined, but it is typically considered to anatomically begin at the point where the atrioventricular nodal tissue enters the central fibrous body. The bundle of His is described as having three regions—the penetrating bundle, nonbranching bundle, and branching bundle. The penetrating bundle is the region that enters the central fibrous body. At this point, the His fascicles are insulated but are surrounded by atrial

Table 13.2 Summary of the histological characteristics of nodal and perinodal tissues in canines

Feature	Atrioventricular bundle (DAVB, His bundle)	Atrioventricular node (AVN)	Proximal atrioventricular bundle (PAVB)
Nucleus	Clear perinuclear zone filled with glycogen	Clear perinuclear zone filled with glycogen	Clear perinuclear zone filled with glycogen
Metabolism	Anaerobic	Anaerobic	Anaerobic
Myofiber size	Largest	Mid	Smallest
Myofibers in fascicles?	Yes	Yes	Yes
Primary fascicles encased in collagen	Yes	Yes	Yes
Secondary fascicles present	Yes	Yes	Yes
Secondary fascicles encased in collagen	Yes	Yes	Yes
Fascicular arrangement	Parallel	Interwoven ("massive whorl")	Parallel
Myofiber arrangement within fascicles	Least spiraling	Spiraled	Most spiraling
Cross striations	Delicate	Delicate	Delicate
End processes present on the myocytes?	Yes. Short and delicate	Yes. Most numerous. Extend from proximal parallel myofibers to central whorled fibers	Yes
Intercalated disks	Broad	Form short stacks	Broadest
Fat vacuoles	Little or none	Little or none	Yes
Vascularization	No large vessels	No large vessels	Large vessels present
Innervation	Tendrils (sympathetic). No packets or fascicles of nerve endings present	Fascicles of boutons, tendrils (sympathetic), and varicosities (parasympathetic) present	Fascicles of boutons, tendrils (sympathetic), and varicosities (parasympathetic) present. Sheaves of nerve endings extend along the length of the myofibers

Compiled from Racker and Kadish [2]

tissue (superiorly and anteriorly), the ventricular septum (inferiorly), and the central fibrous body (posteriorly). Thus, the exact point where the atrioventricular nodal tissues end and the bundle begins is difficult to define, since it occurs over a transitional region. The penetrating bundle has been described as oval in shape and was found to be 1–1.5 mm long in young canines and 0.25–0.75 mm long in neonates [1]. The nonbranching bundle passes through the central fibrous body and is surrounded on all sides by the central fibrous body. In this cardiac region, the His bundle still has atrial tissue superior and anterior to it, the ventricular septum inferior to it, and now the aortic and mitral valves posterior to it. The branching bundle is described to begin as the His exits the central fibrous body. At this point, it is inferior to the membranous septum and superior to the ventricular septum. The bundle is also at its closest proximity to both the right and left ventricular chambers at this point. After leaving the central fibrous body, the bundle then bifurcates into the bundle branches; the right bundle branch passes into the myocardium of the interventricular septum and the left bundle branch travels subendocardially along the septum in the left ventricle. Figures 13.15 and 13.16 show canine histological sections of the bundle of His as they exit the central fibrous body (the branching bundle).

Electrophysiologic studies of the bundle of His commonly have been performed using catheters with polished electrodes and a short interelectrode spacing (i.e., those with diameters of 2 mm). Due to the small amplitude of the His potential, special high-pass filtering must be used (>30 Hz). This high-pass setting must be used in order to separate the His signal from the low-frequency shift in the isopotential line between the atrial depolarization and the atrial repolarization/ventricular depolarization. His potentials can commonly be mapped by deploying an electrode in one of three ways: (1) endocardially in the right atrium at a point on the tricuspid annulus near the membranous septum, (2) epicardially at the base of the aorta near the right atrial appendage, or (3) radially within the noncoronary cusp of the aortic valve [16–18, 20, 45].

Today, His potentials are commonly mapped to provide a landmark for ablation of the atrioventricular node as well as to assess A-to-V conduction timing. In addition to direct electrical mapping, much can be learned about the general anatomical and functional properties of the cells lying within the bundle via attempts to directly stimulate it. For example, direct stimulation of the His produces normal ventricular activation due to the initiation of depolarization into the intrinsic conduction pathway [16, 17, 19]. Thus, if one frequently

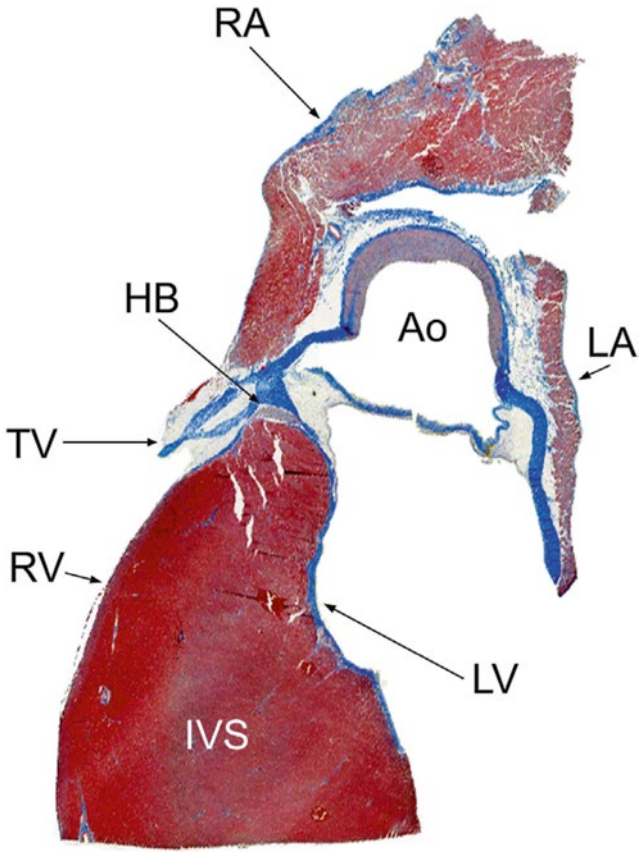

Fig. 13.15 Histologic section through the bundle of His in a canine heart. The section was prepared using a modified Masson's trichrome stain (collagen/nuclei stains *blue*, muscle/keratin/cytoplasm stains *red*). *Ao* aorta, *HB* His bundle, *IVS* interventricular septum, *LA* left atrium, *LV* left ventricular endocardium, *RA* right atrial endocardium, *RV* right ventricular endocardium, *TV* tricuspid valve

experiences failed attempts to selectively stimulate the His bundle, she/he may assume pathological changes [20].

The His bundle has historically been thought to act only as a conduit for transferring depolarization. Ventricular escape rhythms have been known to emanate from the His, but it was considered to be, in general, a relatively simple structure. To the contrary, recent evidence indicates that at least two general sources serve as inputs to the His and that it functions as at least two functionally distinct conduits. Using alternans (alternate beat variation in the direction, amplitude, and duration of any component of the ECG), the duality of its electrophysiology was recently demonstrated in isolated preparations from the region of the triangle of Koch in rabbit hearts [45].

13.7 Comparative Anatomy

All large mammalian hearts are considered to have a very similar conduction system with these main components: sinoatrial node, atrioventricular node, bundle of His, right and left main bundle branches, and Purkinje fibers. Yet, interspecies variations are well recognized [1, 46–48]. For a summary of the major differences in the atrioventricular conduction systems between human, pig, dog, and sheep hearts, refer to Chap. 6.

More specifically, Bharati et al. compared the electrophysiologic properties of the swine and human heart (Table 13.3) [46]. In addition to significant differences in atrial (HRA-LRA) and AV conduction times (much shorter in the swine), the authors also found significantly more autonomic innervation within the atrioventricular node and penetrating bundle of the swine heart (thought to be both adrenergic and cholinergic). They concluded that this indicates a more important neurogenic component to the swine conduction system, relative to the human heart. Due to this difference, they cautioned using swine as a model for assessing cardiac arrhythmias. Although the neurogenic differences between the human and swine are significant in vivo, isolation of such hearts results in denervation of the conduction system and thus reduces or eliminates the relevance of this finding.

The canine is another commonly used model in biomedical device research. Information on A-to-V timing in canines was published by Karpawich et al. [18]. These researchers placed tripolar electrodes on the right atrial epicardium near the noncoronary cusp of the aorta of canines; the resulting timing recorded was extracted from the paper and is tabulated in Table 13.4.

13.8 The Recording of Action Potentials and/or the Spread of Excitation Through the Myocardium

Action potential waveforms can be actively monitored from the epicardial, endocardial, or transmural surfaces of the heart. Several methods exist for the acquisition of such signals, including: (1) glass micropipette electrodes, (2) metal electrodes of various designs, (3) multielectrode arrays, (4) optical mapping, and (5) contact or noncontact endocardial mapping. Contact or noncontact endocardial mapping technologies measure primarily the intracardiac electrograms (endocardial, see also Chap. 32) rather than those from the epicardial surface or globally from the whole myocardium, as in a standard 12-lead ECG. It should be noted that for many ablative arrhythmia therapies, the measurement of intracardiac electrograms within a given cardiac chamber is more common than the recordings from the epicardium (see Chaps. 28 and 29) [49]. Furthermore, algorithms employed by implantable devices such as pacemakers and defibrillators typically use the intercardiac (transmural) electrogram (EGM) signal when detecting an arrhythmia. In this application it is common to use active fixation leads with distal electrodes screwed into the myocardium [50].

Typically, glass micropipettes are produced from small-diameter capillary tubing and then employed for intracellular recordings. These glass tubes are heated (with a burner or

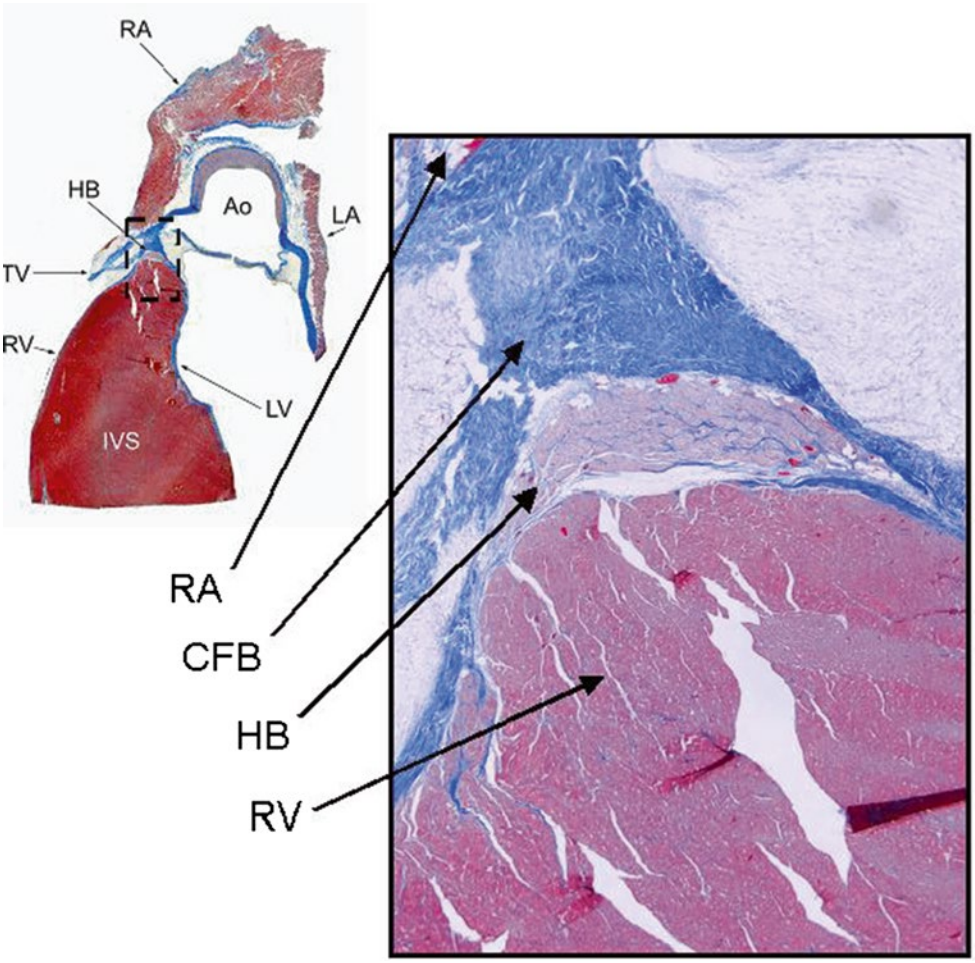

Fig. 13.16 Histologic section through the bundle of His in a canine heart. The region enlarged is noted by the *dashed lines* in the original histologic section. Both sections were prepared using a modified Masson's trichrome stain (collagen/nuclei stain *blue*, muscle/keratin/cytoplasm stain *red*). *Ao* aorta, *CFB* central fibrous body (provides structure and isolates the atrial from the ventricular tissues), *HB* His bundle, *IVS* interventricular septum, *LA* left atrium, *LV* left ventricular endocardium, *RA* right atrial endocardium, *RV* right ventricular endocardium, *TV* tricuspid valve

Table 13.3 Comparison of swine to human electrophysiology

Parameter	Swine (average ± std dev/range)	Normal human
Heart rate (beats per minute)	132 ± 32 (91–167)	60–100
PR interval (ms)	94 ± 27 (50–120)	3–5-year-old: 110–150 5–9-year-old: 120–160
QT interval (ms)	256 ± 69 (150–340)	HR = 150: 210–280 HR = 100: 260–350
HRA-LRA (ms)	10 ± 0 (10)	2–5-year-old: 6–38 6–10-year-old: 0–41
LRA-H (ms)	63 ± 2 (60–65)	2–5-year-old: 45–101 6–10-year-old: 40–124
H-V (ms)	25 ± 7 (20–35)	2–5-year-old: 27–59 6–10-year-old: 28–52

H His, *HR* heart rate, *HRA* high right atrium, *LRA* low right atrium, *V* ventricle

Adapted from Bharati et al. [46]

Table 13.4 Tabulation of activation timing

	P-wave to R-wave interval (ms)	Atrial activation to His bundle electrogram (ms)	His bundle electrogram to ventricular activation (ms)
Mean	92.1	77.5	29
Std Dev	18.4	11.5	8.9
Max	120	100	50
Min	70	60	20

Data compiled from Karpawich et al. [18]

heating element) and then, under tension, elongated (stretched) to produce a constriction that eventually breaks. Currently, this process is typically facilitated by a commercially available micropipette puller which reproducibly creates electrodes with tips of about 0.1 μm with resistances of 10–40 MΩ. The pipette is then filled with an electrolyte such as 3M KCl. A silver, platinum, or stainless steel wire is then positioned inside the pipette until it is in contact with the electrolytic solution [51]. The user must be careful manipulating the fragile electrode tip, especially when recording directly from a beating, moving cell. The ultimate goal of this recording approach is to impale the microelectrode through the cell membrane, so that the tip is into the myoplasm of a single cell while not inducing major damage to the cell; the membrane seals around the tip and the cell does not become depolarized.

There are various designs for metal recording electrodes which can be employed to monitor action potential wave-

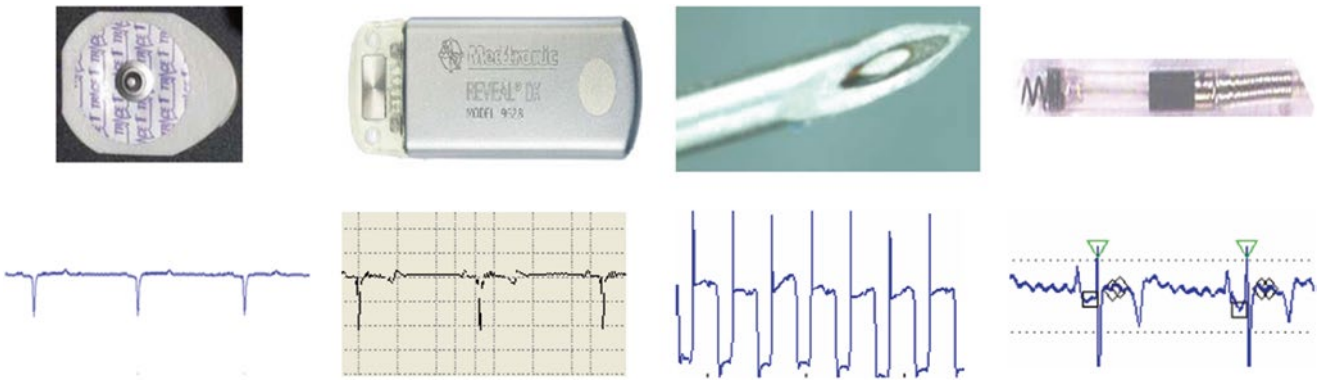

Fig. 13.17 Representative cardiac signals. The leftmost signal is from a standard Ag/AgCl surface electrode. The second signal was collected subcutaneously with a Medtronic Reveal® Dx insertable cardiac monitor (Medtronic, Inc, Minneapolis, MN, USA). The third signal was collected from a concentric bipolar needle electrode with 0.3 mm spacing between conductors. The last endocardial signal was obtained with a Medtronic 5076 screw-in electrode in the right ventricle; this electrogram has key fiducial points marked

forms extracellularly. One of the most common methods is to use a needle with two closely spaced embedded conductors. Yet, the relative spacing between the active and reference conductors can be manipulated to control the sensing area [52]. Another method is to use an internal conductor needle with the cannula of the needle as the reference electrode. In such cases, the internal conducting wire is electrically isolated from the cannula. In a monopolar configuration, the needle is a single shaft, and the reference is taken from the subject ground. Each of these designs can have needle tip diameters as small as 0.30 mm.

Various types of electrode designs and typical signals that can be recorded with each are shown in Fig. 13.17. Note that the morphology of a recorded signal will typically depend on: (1) the configuration of the electrode employed (monopolar/unipolar or bipolar), (2) the relative surface area that the electrode will monitor, (3) the anatomical placement (atrium or ventricle), and/or (4) the site-specific myocardial wall recording location (endocardial, epicardial, or transmural). Multiple ECG patches, for example, are used to cover a larger surface area on the skin and thus detect potential changes from a large transmural field, whereas a bipolar concentric needle placed epicardially records from a focal population of cells. In other words, the surface electrodes will provide a signal representative of a major portion of the whole heart, while the small bipolar needle electrode provides a much more localized signal.

Active and passive pacing leads can be used to detect action potential waveforms, commonly used today in either unipolar or bipolar configurations (i.e., with those leads that have both a distal-tip electrode and a distal-ring electrode). Such leads can be used for either sensing or pacing. Modern pacemaker lead diameters range from 4 to 10 French (1 French = one-third millimeter). Note, their relative dimensions will ultimately dictate the size of the field from which they are sensing electrical potentials. As with any active fixation lead or metal electrode which is engaged into the myocardium, an initial injury potential can be associated with its placement [53]. The current trend in the pacing lead industry is to continually decrease the diameter of both the body and tip dimensions (i.e., 2 Fr leads are currently in development and clinical trials).

One can consider that an extension of the single-electrode approach is the multielectrode array. As the name implies, such systems consist of an array of equally spaced electrodes supported by a base. Conducting wires are attached to the electrodes on the array. Depending on the design, one or more of the electrodes on the array can serve as the reference electrode, while the others become the active electrodes. These arrays allow for the mapping of electrical potentials within a given region of the heart [54]. The designer or eventual user must determine the appropriate electrode spacing for a given application while also considering the relative electrode configurations, employed sampling rates, and/or density of electrodes necessary to elucidate or monitor the nature of the desired local events.

Catheter-based cardiac mapping systems are primarily used to understand the underlying mechanisms of arrhythmias. In principle, electroanatomical mapping systems use low magnetic fields to reconstruct 3D maps and electrical activation sequences of the chamber of interest. Briefly, in sequential mapping systems, mapping catheters with radiofrequency capability are placed into the heart chamber with fluoroscopic guidance. Low magnetic fields are generated by pads located under the patient's bed. The sensor tip of the catheter attains data in order to compute information regarding magnetic field amplitude, frequency, and phase to reconstruct a spatial 3D position. After chamber reconstruction, sequential recording of electrical activation is recorded by dragging the catheter along the endocardial wall. The intercardiac electrogram is measured and typically the activation time is superimposed on the reconstructed 3D chamber,

resembling a contour map. The reconstruction process can be conducted in real time; however, the process is time consuming since it is a sequential process. Using these methods, one can gain insights on the relative spread of excitation through a given chamber or portions of the conduction system.

Contact mapping can also be conducted with basket catheters that typically contain 32–64 nickel or titanium electrodes that are 1–2 mm long and 1 mm in diameter with interelectrode distances from 3 to 10 mm. The endocardial surface is mapped at the basket's splines, making contact with the chamber wall. This technique has limitations, however, since a catheter that is too small or too large will result in poor-quality electrogram recordings. The technique is also susceptible to movement artifacts from the continuously beating heart [55, 56]. Nevertheless, one can track relative electrical activities through the heart with these methodologies.

Another approach to 3D chamber mapping is noncontact mapping technology. One such product is the EnSite® system manufactured by Endocardial Solutions (St. Jude Medical, St. Paul, MN, USA). This system includes a catheter with 64 laser-etched unipolar electrodes that lies within the chamber; one can track, on a beat-to-beat basis, the activation and repolarization patterns in a given chamber (see Chap. 32 for more details on these systems and new non-invasive mapping technologies). It is the continued development of cardiac mapping systems that helps physicians localize sites for catheter ablation for the treatment of complex cardiac arrhythmias such as tachycardia or atrial fibrillation [55, 57]. Catheters used for noncontact cardiac mapping of endocardial activation and repolarization processes are typically 9 Fr in diameter.

13.9 Future Research

Although much is already known, a great deal of supposition and controversy remains related to our understanding of the cardiac conduction system. Specifically, characterization of the anatomy and electrophysiology of the atrioventricular nodal region and the bundle of His continues to be an area of great scientific interest and debate [58–60]. For example, current clinical interest in the atrioventricular node and His bundle has focused research on their potential stimulation to ultimately improve hemodynamics in patients requiring pacing [16–21], as well as their use in treating atrioventricular nodal reentrant tachycardias [1, 2, 54, 61]. Also, there is increasing evidence about the critical role that cardiac innervation plays in the control and modulation of rhythms, including evidence of ganglia in the pulmonary vein sleeves modulating the rate of the sinus node [62]. A new cell type has also been discovered in the pulmonary vein sleeves, in the atrial tissue, and in the ventricular myocardium. These interstitial Cajal-like cells (*telocytes*) are leading to new hypotheses regarding the origins of rhythms, arrhythmias, and coordination of intercellular signaling [63–66]. In addition to a potential source of arrhythmias, these cells may prove to be an additional source of the ventricular rescue rhythms. Future scientific investigations will serve to improve our understanding of the fundamental physiology of the heart's conduction system and the mechanisms of cardiac activation in normal and diseased tissues. The findings from these studies will provide a better foundation for future therapies. For additional reviews on the human cardiac conduction system, the reader is referred to those by Iaizzo and Laske [67], Dobrzynski et al. [68], and Anderson et al. [69].

13.10 Summary

This chapter reviewed the basic architecture and function of the cardiac conduction system in order to provide the reader with a working knowledge and vocabulary related to this topic. While a great deal of literature exists regarding the cardiac conduction system, numerous questions remain related to the detailed histological anatomy and cellular physiology of these specialized conduction tissues and how they become modified in disease states. Future findings associated with the function and anatomy of the cardiac conduction system will likely lead to improvements in therapeutic approaches and medical devices.

Acknowledgments We would like to thank Medtronic Training and Education and Gorinka Shrivastav for graphical support; Rebecca Rose, DVM, Louanne Cheever, and Alexander Hill, PhD, of Medtronic for the histological sectioning and staining; Anthony Weinhaus, PhD, for additional details on atrial anatomy; and Igor Efimov, PhD, from George Washington University for 3D images of the human atrioventricular node.

References

1. Ho SY, Kilpatrick L, Kanai T et al (1995) The architecture of the atrioventricular conduction axis in dog compared to man–its significance to ablation of the atrioventricular nodal approaches. J Cardiovasc Electrophysiol 6:26–39
2. Racker DK, Kadish AH (2000) Proximal atrioventricular bundle, atrioventricular node, and distal atrioventricular bundle are distinct anatomic structures with unique histological characteristics and innervation. Circulation 101:1049–1059
3. Furman S (1995) A brief history of cardiac stimulation and electrophysiology – the past fifty years and the next century. NASPE Keynote Address
4. Boyett D, Dobrzynski H (2007) The sinoatrial node is still setting the pace 100 years after its discovery. Circ Res 100:1543–1545
5. His W Jr (1893) Die Tatigkeit des embryonalen herzens und deren bedcutung fur die lehre von der herzbewegung beim erwachsenen. Artbeiten aus der Medizinischen Klinik zu Leipzig 1:14–49
6. Tawara S (1906) Das Reizleitungssystem des Saugetierherzens: Eine anatomisch-histologische Studie uber das Atrioventrikularbundel und die Purkinjeschen Faden. Gustav Fischer, Jena, pp 9–70, 114–156

7. Conti AA, Giaccardi M, Yen Ho S, Padeletti L (2006) Koch and the "ultimum moriens" theory – the last part to die of the heart. J Interv Card Electrophysiol 15:69–70
8. Koch WK (1922) Der funktionelle bau des menschlichen herzen. Urban und Schwarzenberg, Berlin and Vienna
9. Sorensen ER, Manna D, McCourt K (1994) Use of epicardial pacing wires after coronary artery bypass surgery. Heart Lung 23:487–492
10. Villain E, Ouarda F, Beyler C, Sidi D, Abid F (2003) Predictive factors for late complete atrioventricular block after surgical treatment for congenital cardiopathy. Arch Mal Coeur Vaiss 96:495–498
11. Bae EJ, Lee JY, Noh CI, Kim WH, Kim YJ (2003) Sinus node dysfunction after Fontan modifications—influence of surgical method. Int J Cardiol 88:285–291
12. Hussain A, Malik A, Jalal A, Rehman M (2002) Abnormalities of conduction after total correction of Fallot's Tetralogy: a prospective study. J Pak Med Assoc 52:77–82
13. Bruckheimer E, Berul CI, Kopf GS et al (2002) Late recovery of surgically-induced atrioventricular block in patients with congenital heart disease. J Interv Card Electrophysiol 6:191–195
14. Ghosh PK, Singh H, Bidwai PS (1989) Complete A-V block and phrenic paralysis complicating surgical closure of ventricular septal defect-A case report. Indian Heart J 41:335–337
15. Hill SL, Berul CI, Patel HT, Rhodes J, Supran SE, Cao QL, Hijazi ZM (2000) Early ECG abnormalities associated with transcatheter closure of atrial septal defects using the Amplatzer Septal Occluder. J Interv Card Electrophysiol 4:469–474
16. Deshmukh P, Casavant DA, Romanyshyn M, Anderson K (2000) Permanent direct His-bundle pacing: a novel approach to cardiac pacing in patients with normal His-Purkinje activation. Circulation 101:869–877
17. Karpawich P, Gates J, Stokes K (1992) Septal His-Purkinje ventricular pacing in canines: a new endocardial electrode approach. Pacing Clin Electrophysiol 15:2011–2015
18. Karpawich PP, Gillette PC, Lewis RM, Zinner A, McNamera DG (1983) Chronic epicardial His bundle recordings in awake nonsedated dogs: a new method. Am Heart J 105:16–21
19. Scheinman MM, Saxon LA (2000) Long-term His-bundle pacing and cardiac function. Circulation 101:836–837
20. Williams DO, Sherlag BJ, Hope RR, El-Sherif N, Lazzara R, Samet P (1976) Selective versus non-selective His bundle pacing. Cardiovasc Res 10:91–100
21. Karpawich PP, Rabah R, Haas JE (1999) Altered cardiac histology following apical right ventricular pacing in patients with congenital atrioventricular block. Pacing Clin Electrophysiol 22:1372–1377
22. de Cock CC, Giudici MC, Twisk JW (2003) Comparison of the haemodynamic effects of right ventricular outflow-tract pacing with right ventricular apex pacing: a quantitative review. Europace 5:275–278
23. Cleland JG, Daubert JC, Erdmann E et al (2001) The CARE-HF study (CArdiac REsynchronisation in Heart Failure study): rationale, design and end-points. Eur J Heart Fail 3:481–489
24. Leclercq C, Daubert JC (2003) Cardiac resynchronization therapy is an important advance in the management of congestive heart failure. J Cardiovasc Electrophysiol 14:S27–S29
25. Rosen MR (2014) Gene therapy and biological pacing. N Engl J Med 371:1158–1159
26. Nattel S, Khairy P, Roy D et al (2002) New approaches to atrial fibrillation management: a critical review of a rapidly evolving field. Drugs 62:2377–2397
27. Takahashi Y, Yoshito I, Takahashi A et al (2003) AV nodal ablation and pacemaker implantation improves hemodynamic function in atrial fibrillation. Pacing Clin Electrophysiol 26:1212–1217
28. Bernat R, Pfeiffer D (2003) Long-term Rand learning curve for radio frequency ablation of accessory pathways. Coll Antropol 27:83–91
29. Gaita F, Riccardi R, Gallotti R (2002) Surgical approaches to atrial fibrillation. Card Electrophysiol Rev 6:401–405
30. Betts TR, Roberts PR, Ho SY, Morgan JM (2003) High density mapping of shifts in the site of earliest depolarization during sinus rhythm and sinus tachycardia. Pacing Clin Electrophysiol 26:874–882
31. Boineau JB, Schuessler RB, Hackel DB et al (1980) Widespread distribution and rate differentiation of the atrial pacemaker complex. Am J Physiol 239:H406–H415
32. Boineau JB, Schuessler RB, Mooney CR (1978) Multicentric origin of the atrial depolarization wave: the pacemaker complex. Relation to the dynamics of atrial conduction, P-wave changes and heart rate control. Circulation 58:1036–1048
33. Lee RJ, Kalman JM, Fitzpatrick AP et al (1995) Radiofrequency catheter modification of the sinus node for 'inappropriate' sinus tachycardia. Circulation 92:2919–2928
34. Tranum-Jensen J (1976) The fine structure of the atrial and atrioventricular (AV) junctional specialized tissues of the rabbit heart. In: Wellens HJJ, Lie KI, Janse MJ (eds) The conduction system of the heart: structure, function, and clinical implications. Lea & Febiger, Philadelphia, pp 55–81
35. Waller BF, Gering LE, Branyas NA, Slack JD (1993) Anatomy, histology, and pathology of the cardiac conduction system: Part I. Clin Cardiol 16:249–252
36. Boyett MR, Honjo H, Kodama I et al (2007) The sinoatrial node: cell size does matter. Circ Res 101:e81–e82
37. Garson AJ, Bricker JT, Fisher DJ, Neish SR (eds) (1998) The science and practice of pediatric cardiology, vol I. Williams & Williams, Baltimore, pp 141–143
38. Hucker WJ, Fedorov VV, Foyil KV, Moazami N, Efimov IR (2008) Optical mapping of the human atrioventricular junction. Circulation 117:1474–1477
39. Li JL, Greener ID, Inada S et al (2008) Computer three-dimensional reconstruction of the atrioventricular node. Circ Res 102:975–985
40. Becker AE, Anderson RH (1976) The morphology of the human atrioventricular junctional area. In: Wellens HJJ, Lie KI, Janse MJ (eds) The conduction system of the heart: structure, function, and clinical implications. Lea & Febiger, Philadelphia, pp 263–286
41. Aschoff L (1910) Referat uber die herzstorungen in ihren bezeihungen zu den spezifischen muskelsystem des herzens. Verh Dtsch Ges Pathol 14:3–35
42. Monckeberg JG (1910) Beitrage zur normalen und pathologischen anatomie des herzens. Verh Dtsch Ges Pathol 14:64–71
43. Hucker WJ, McCain ML, Laughner JI, Iaizzo PA, Efimov IR (2008) Connexin 43 expression delineates two discrete pathways in the human atrioventricular junction. Anat Rec 291:204–215
44. Davis LM, Rodefeld ME, Green K, Beyer EC, Saffitz JE (1995) Gap junction protein phenotypes of the human heart and conduction system. J Cardiovasc Electrophysiol 6:813–822
45. Zhang Y, Bharati S, Mowrey KA, Shaowei Z, Tchou PJ, Mazgalev TN (2001) His electrogram alternans reveal dual-wavefront inputs into and longitudinal dissociation within the bundle of His. Circulation 104:832–838
46. Bharati S, Levine M, Huang SK et al (1991) The conduction system of the swine heart. Chest 100:207–212
47. Anderson RH, Becker AE, Brechenmacher C, Davies MJ, Rossi L (1975) The human atrioventricular junctional area. A morphological study of the A-V node and bundle. Eur J Cardiol 3:11–25
48. Frink RJ, Merrick B (1974) The sheep heart: coronary and conduction system anatomy with special reference to the presence of an os cordis. Anat Rec 179:189–200
49. El-Sherif N, Lekieffre J (1997) Practical management of cardiac arrhythmias. Futura Publishing Co., Armonk, p 348
50. Shrivastav M, Iaizzo P (2007) Discrimination of ischemia and normal sinus rhythm for cardiac signals using a modified k means clustering algorithm. Conf Proc IEEE Eng Med Biol Soc, 3856–3859
51. Webster JG (2004) Bioinstrumentation. Wiley, Hoboken, p 383

52. Shrivastav M (1999) Methods of ambulatory detection and treatment of cardiac arrhythmias using implantable cardioverter-defibrillators. Biomed Instrum Technol 33:505–521
53. Webster JG (ed) (1995) Design of cardiac pacemakers. IEEE Press, Piscataway
54. Sahakian AV, Peterson MS, Shkurovich S et al (2001) A simultaneous multichannel monophasic action potential electrode array for in vivo epicardial repolarization mapping. IEEE Trans Biomed Eng 48:345–353
55. Shenasa M, Borggrefe M, Breithardt G (eds) (2003) Cardiac mapping, 2nd edn. Futura, New York, p 784
56. Shrivastav M, Iaizzo PA (2006) In vivo cardiac monophasic action potential recording using electromyogram needles. In: Proceedings of the IEEE biomedical circuits and systems conference, London
57. Schilling RJ, Kadish AH, Peters NS, Goldberger J, Davies DW (2000) Endocardial mapping of atrial fibrillation in the human right atrium using a non-contact catheter. Eur Heart J 21:550–564
58. Becker AE, Anderson RH (2001) Proximal atrioventricular bundle, atrioventricular node, and distal atrioventricular bundle are distinct anatomic structures with unique histological characteristics and innervation – response. Circulation 103:e30–e31
59. Bharati S (2001) Anatomy of the atrioventricular conduction system – response. Circulation 103:e63–e64
60. Magalev TN, Ho SY, Anderson RH (2001) Special Report: Anatomic-electrophysiological correlations concerning the pathways for atrioventricular conduction. Circulation 103:2660–2667
61. Kucera JP, Rudy Y (2001) Mechanistic insights into very slow conduction in branching cardiac tissue – a model study. Circulation Res 89:799–806
62. Zarzoso M, Rysevaite K, Milstein ML et al (2013) Nerves projecting from the intrinsic cardiac ganglia of the pulmonary veins modulate sinoatrial node pacemaker function. Cardiovasc Res 99:566–575
63. Hinescu ME, Popescu LM (2005) Interstitial Cajal-like cells (ICLC) in human atrial myocardium. J Cell Mol Med 9:972–975
64. Kostin S (2010) Myocardial telocytes: a specific new cellular entity. J Cell Mol Med 14:1917–1921
65. Gherghiceanu M, Popescu LM (2012) Cardiac telocytes – their junctions and functional implications. Cell Tissue Res 348:265–279
66. Cretoiu SM, Popescu LM (2014) Telocytes revisited. Biomol Concepts 5:353–369
67. Iaizzo PA, Laske TG (2010) Anatomy and physiology of the cardiac conduction system. In: Sigg DC, Iaizzo PA (eds) Cardiac electrophysiology methods and models. Springer, New York, pp 73–90
68. Dobrzynski H, Anderson RH, Atkinson A et al (2013) Structure, function and clinical relevance of the cardiac conduction system, including the atrioventricular ring and outflow tract tissues. Pharmacol Ther 139:260–288
69. Anderson RH, Boyett MR, Dobrzynski H, Moorman AF (2013) The anatomy of the conduction system: implications for the clinical cardiologist. J Cardiovasc Transl Res 6:187–196

Further Reading

Mohrman DE, Heller LJ (eds) (2003) Cardiovascular physiology, 5th edn. Langer Medical Books/McGraw-Hill, New York

Wellens HJJ, Lie KI, Janse MJ (eds) (1976) The conduction system of the heart: structure, function, and clinical implications. Lea & Febiger, Philadelphia

Alexander RW, Schlant RC, Fuster V (eds) (1998) Hurst's the heart: arteries and veins, 9th edn. McGraw-Hill, New York

Katz AM (ed) (2001) Physiology of the heart, 3rd edn. Lippincott, Williams, and Wilkins, Philadelphia

Tortora GJ, Grabowski SR (eds) (2000) Principles of anatomy and physiology, 9th edn. Wiley, New York